Phenomenological study of the angle between jet axes in heavy-ion collisions

Jin-Wen Kang

Institute of Particle Phisics
Central China Normal University

HF-HNC 2024, Guangzhou, China
December 06–11, 2024

J. W. Kang, S. Wang, L. Wang, B. W. Zhang, arXiv:2312.15518 [hep-ph]

Outline

Heavy-ion Collisions and Jet Quenching

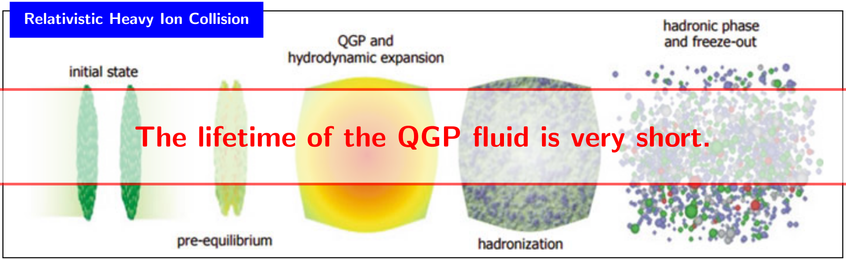

The lifetime of the QGP fluid is very short.

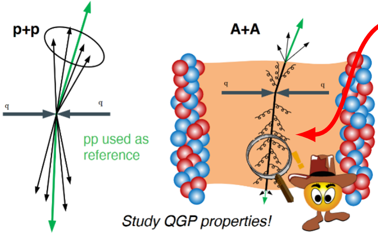

energy loss: $\frac{\mathrm{d}E}{\mathrm{d}t}$, p_T-broadening: $\frac{\mathrm{d}p_\perp}{\mathrm{d}t}$

During the propagation and evolution in the QGP, the jet not only loses energy and momentum, but also accumulates p_T-broadening through medium-induced radiation and scattering.

Probing Intra-Broadening by Jet Substructures

$$\Delta R^{a-b}_{\mathrm{axis}} = \sqrt{\left(y^{a}_{\mathrm{axis}} - y^{b}_{\mathrm{axis}}\right)^2 + \left(\phi^{a}_{\mathrm{axis}} - \phi_{\mathrm{axis}^b}\right)^2}$$

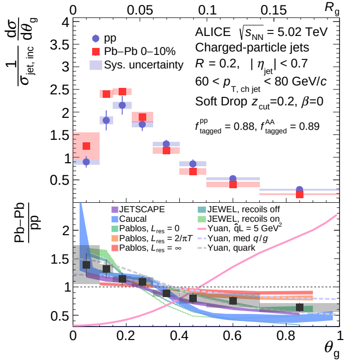

ALICE, Phys. Rev. Lett. **128**, 102001 (2022)

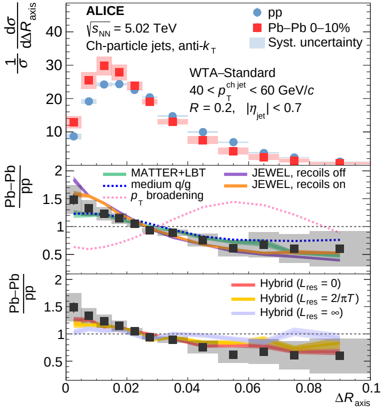

ALICE, arXiv:2303.13347 [nucl-ex]

Measurements seem to discard intra-jet broadening.

Angle Between Jet Axes

$$\Delta R^{a-b}_{\text{axis}} = \sqrt{\left(y^a_{\text{axis}} - y^b_{\text{axis}}\right)^2 + \left(\phi^a_{\text{axis}} - \phi_{\text{axis}^b}\right)^2} \quad (1)$$

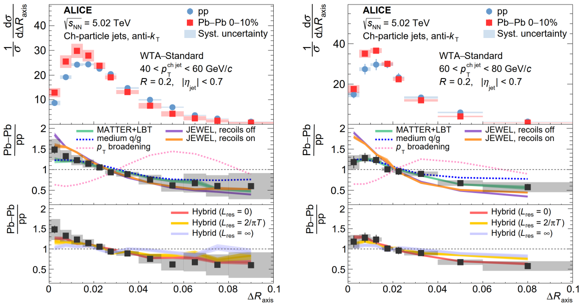

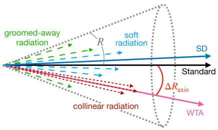

ALICE, arXiv:2303.13347 [nucl-ex]

$$\Delta R_{\text{axis}}^{a-b} = \sqrt{\left(y_{\text{axis}}^{a} - y_{\text{axis}}^{b}\right)^2 + \left(\phi_{\text{axis}}^{a} - \phi_{\text{axis}^b}\right)^2} \qquad (1)$$

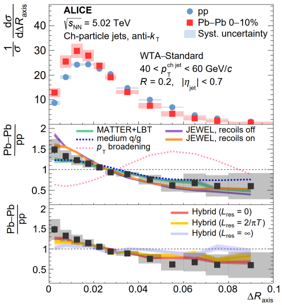

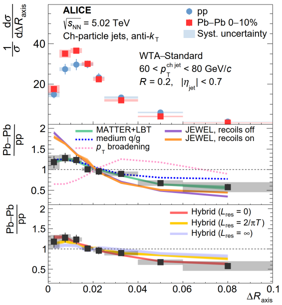

ALICE, arXiv:2303.13347 [nucl-ex]

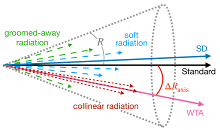

Standard axis: anti-k_t algorithm + E-scheme
WTA axis: C/A algorithm + WTA-scheme

WTA (winner-take-all) recombination scheme:

$$p_{T,r} = p_{T,1} + p_{T,2},\ x_r = \begin{cases} x_1 & \text{if } p_{T,1} > p_{T,2} \\ x_2 & \text{if } p_{T,1} < p_{T,2} \end{cases}$$

x_a is the y, ϕ of the sub-jet a.

WTA's Features

- collinear/infra-red safety
- powerfully suppress the effect of soft radiation

The WTA axis is typically aligned with the most energetic components of the jet.

Angle Between Jet Axes

华中师范大学 CENTRAL CHINA NORMAL UNIVERSITY

$$\Delta R^{a-b}_{\rm axis} = \sqrt{\left(y^{a}_{\rm axis} - y^{b}_{\rm axis}\right)^2 + \left(\phi^{a}_{\rm axis} - \phi_{{\rm axis}^{b}}\right)^2} \quad (1)$$

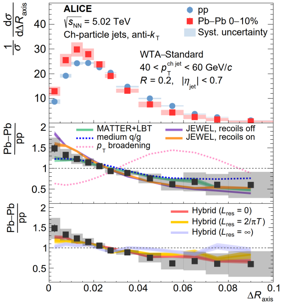

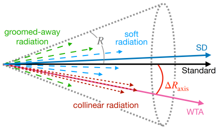

Standard axis: anti-k_t algorithm + E-scheme
WTA axis: C/A algorithm + WTA-scheme

WTA (winner-take-all) recombination scheme:

$$p_{T,r} = p_{T,1} + p_{T,2}, \; x_r = \begin{cases} x_1 & \textbf{if } p_{T,1} > p_{T,2} \\ x_2 & \textbf{if } p_{T,1} < p_{T,2} \end{cases}$$

x_a is the y, ϕ of the sub-jet a.

ALICE's Conclusions

ALICE, arXiv:2303.13347 [nucl-ex]

- Narrowing of the $\Delta R_{\rm axis}$ distribution relative to the vacuum case.
- **The narrowing may be explained if the Pb-Pb distribution is dominated by quark-initiated jets.**
- The narrowing may be due to a selection bias.
- Measurements discard intra-jet p_T broadening.

WTA's Features

- collinear/infra-red safety
- powerfully suppress the effect of soft radiation

The WTA axis is typically aligned with the most energetic components of the jet.

Angle Between Jet Axes

$$\Delta R^{a-b}_{\text{axis}} = \sqrt{\left(y^a_{\text{axis}} - y^b_{\text{axis}}\right)^2 + \left(\phi^a_{\text{axis}} - \phi_{\text{axis}^b}\right)^2} \quad (1)$$

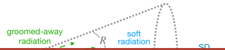

Our Issues

- The fraction of quark-initiated jets increases after jet quenching, but it is far from dominant.

quark jet fraction	p+p	Pb+Pb
inclusive jets	33%	45%
Z^0 tagged jets	88%	92%

TABLE I: Estimation of quark jet fraction of inclusive jets and Z^0 tagged jets in p+p and Pb+Pb collisions at leading-order (LO), with jet radius $R = 0.2$, 40 GeV $< p_{T,\text{jet}} <$ 60 GeV.

Yan *et al.*, Chin. Phys. C **45**, no.2, 024102 (2021)

- What role does selection bias play?
- Why were the measurements unable to detect intra-jet p_T broadening?

ALICE's Conclusions

- collinear/infra-red safety
- powerfully suppress the effect of soft radiation

- **The narrowing may be explained if the Pb-Pb distribution is dominated by quark-initiated jets.**
- The narrowing may be due to a selection bias.
- Measurements discard intra-jet p_T broadening.

The WTA axis is typically aligned with the most energetic components of the jet.

Framework

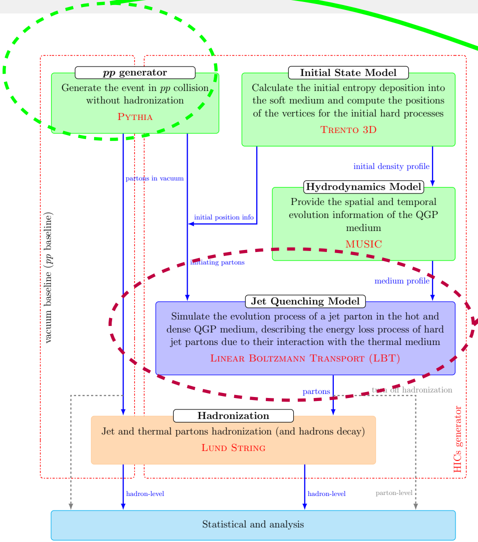

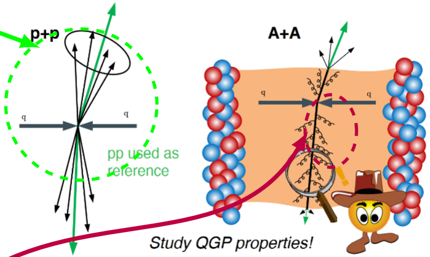

- $p+p$ baseline: PYTHIA8
  T. Sjöstrand *et al.*, COMPUT. PHYS. COMMUN. **191**, 159 (2015)
- Initial state: TRENTO 3D (averaged)
  W. Ke *et al.*, PHYS. REV. C **96**, no.4, 044912 (2017)
- Partonic transport in the QGP: LBT
  PLB 782 (2018) 707; PRC 98 (2018) 021901; PLB 777 (2018) 86; PRC 94 (2016) 014909
- Hydrodynamic evolution: MUSIC
  PRC 82, 014903 (2010); PRL 106, 042301 (2011); PRC 93, 044906 (2016)
- Hadronization: COLORLESS

ARXIV:1903.07706 [hep-ph]

LBT Model

the phase space distribution of a jet parton a

$$p_a^\mu \partial_\mu f_a = E_a \cdot C_a^{\text{el+inel}}$$

the sum of collision integrals for (in)elastic

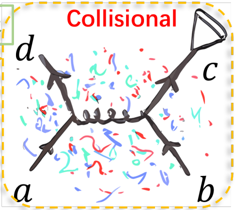

PLB 782 (2018) 707-716; PRC 98 (2018) 021901; PLB 777 (2018) 86; PRC 94 (2016) 014909.

For a hard parton a scattering with a thermal parton b via a specific channel $ab \to cd$,

$$\Gamma^{\text{el}}_{ab\to cd} = \frac{g_b}{2E_a} \int \prod_{i=bc,d} \mathrm{d}[p_i] f_b(E_b, T) S_2(\hat{s}, \hat{t}, \hat{u}) (2\pi)^4 \delta^{(4)} \left|\mathcal{M}_{ab\to cd}\right|^2. \quad (2)$$

Jet transport coefficient:

$$\hat{q}_a = \left\langle q_\perp^2/\lambda \right\rangle_a = \sum_{b,(cd)} \int_{\mu_D^2}^{s/4} \mathrm{d}q_\perp^2 \frac{\mathrm{d}\sigma_{ab\to cd}}{\mathrm{d}q_\perp^2} \rho_b q_\perp^2. \quad (3)$$

LBT Model – Radiative Eloss Mechanisms

The inelastic scattering rate relates to the average number of emitted gluons from parton a per unit time,

$$\Gamma_a^{\mathrm{inel}}(E_a, T, t) = \frac{1}{1+\delta_g^a} \int \mathrm{d}z \, \mathrm{d}k_\perp^2 \frac{\mathrm{d}N_g^a}{\mathrm{d}k_\perp^2 \, \mathrm{d}t}. \tag{4}$$

The medium-induced gluon spectrum is taken from the high-twist energy loss calcumation, PRL 85 (2000) 3591, PRL 93 (2004) 072301, PRD 93 (2004) 072301.

$$\frac{\mathrm{d}N_g^a}{\mathrm{d}z \, \mathrm{d}k_\perp^2 \, \mathrm{d}t} = \frac{2 C_A \alpha_s \hat{q}_a P_a^{\mathrm{vac}}(z) k_\perp^4}{\pi \left(k_\perp^2 + z^2 m^2\right)} \sin^2\left(\frac{t - t_i}{2\tau_f}\right)$$

the parent parton a
the parton transport coefficient
the vacuum splitting function
the production time of parton a
the transverse momentum of the emitted gluon
the mass of parton a
the fractional energy of the emitted gluon
the formation time of the emitted gluon, $\tau_f = 2E_a z(1-z)/\left(k_\perp^2 + z^2 m^2\right)$

Model Validation

Event Selection

- Reconstructed from tracks with $p_{\mathrm{T,track}} > 0.15$ GeV, $|\eta| < 0.9$
- Using the anti-k_t algorithm with E-scheme recombination for resolution parameters $R = 0.2$
- $40 < p_{\mathrm{T,jet}} < 60$ GeV, $|\eta_{\mathrm{jet}}| < 0.7$.

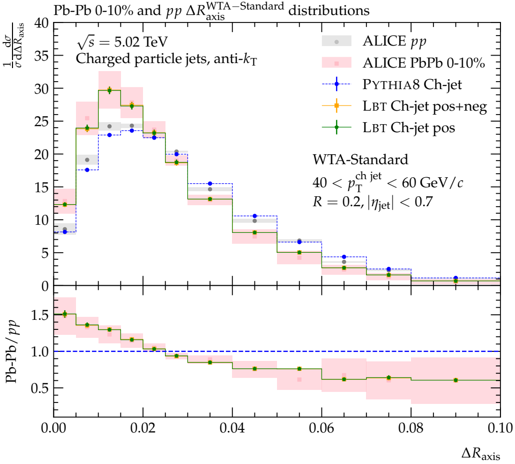

Figure: Distributions of the angle ΔR_{axis} in p+p and Pb+Pb collisions.

Model Validation

Event Selection

- Reconstructed from tracks with $p_{\mathrm{T,track}} > 0.15$ GeV, $|\eta| < 0.9$
- Using the anti-k_t algorithm with E-scheme recombination for resolution parameters $R = 0.2$
- $40 < p_{\mathrm{T,jet}} < 60$ GeV, $|\eta_{\mathrm{jet}}| < 0.7$.

✓ The angle between the Standard and WTA jet axes is not sensitive to the medium response, at least when $R = 0.2$.

✓ Reasonably describe the experimental data in both p+p and Pb+Pb collisions and the PbPb/pp ratio.

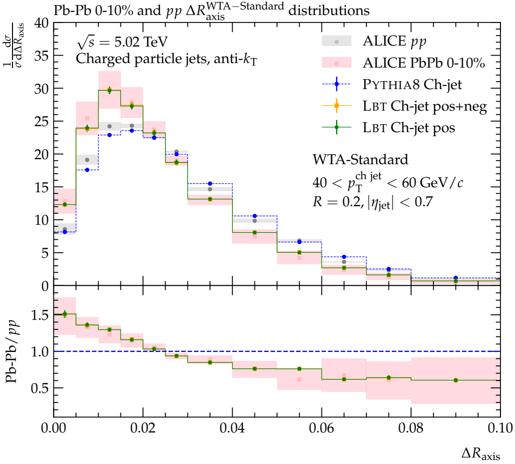

Figure: Distributions of the angle ΔR_{axis} in p+p and Pb+Pb collisions.

Selection Bias in Jet Quenching

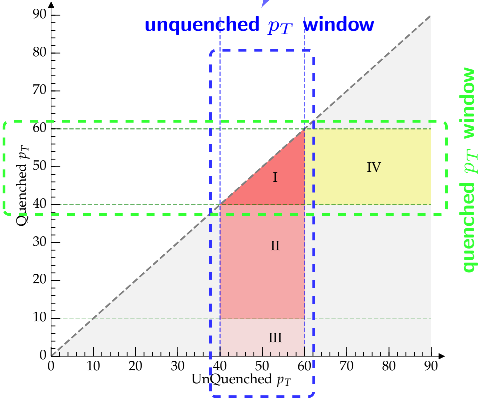

Figure: Schematic diagram of the selection bias due to jet energy loss that may occur when selecting jets based on the their transverse momentum.

General Selected Regions:

- **UnQuenched:** I+II+III
- **Quenched :** I+IV

⚠ *We have overlooked the possibility of new jet production within the medium.*

◀ **Note:** The horizontal axis corresponds to the transverse momentum of the unquenched jets, and the vertical axis corresponds to the quenched jets' transverse momentum. Effective jets exist only in the shaded area of the lower triangle.

華中師範大學 CENTRAL CHINA NORMAL UNIVERSITY

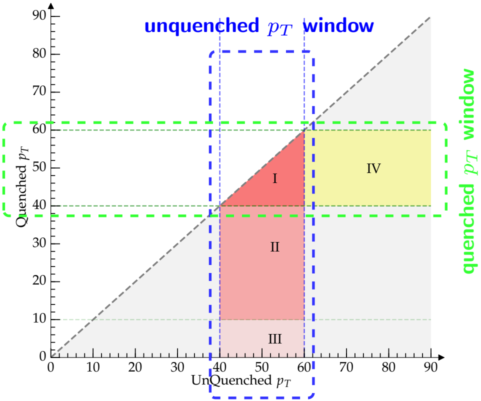

Figure: Schematic diagram of the selection bias due to jet energy loss that may occur when selecting jets based on the their transverse momentum.

General Selected Regions:

- **UnQuenched:** I+II+III
- **Quenched :** I+IV

Method of Jet-by-Jet Matching

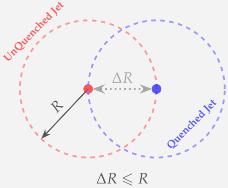

In paired quenched and unquenched events, jets are reconstructed separately, then the angular distances between the unquenched jet and all quenched jets are calculated, respectively, and the closest one is selected as the quenched jet corresponding to the unquenched jet.

Our Selected Regions:

- **UnQuenched:** I+II
- **Quenched :** I+II

arXiv:2009.03316 [hep-ph]

First Select, then Quench. So called "Select-then-Quench" (STQ).

Influence of Selection Bias

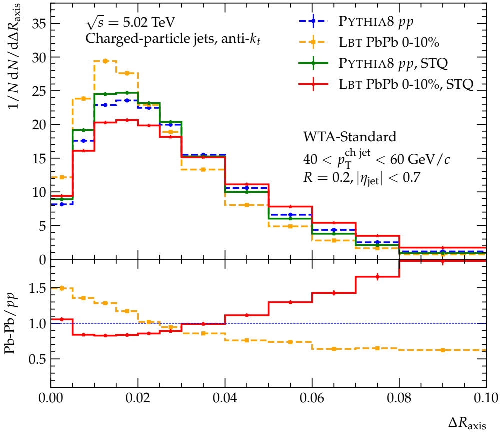

arXiv:2312.15518 [hep-ph]

Figure: Normalized ΔR_{axis} distribution of the selected jet samples in p+p and Pb+Pb collisions.

Conclusions:

- The ΔR_{axis} distribution of STQ (PbPb) shows evident broadening compared to that of STQ (pp).
- It means the jets get broader by the interactions with the QGP medium compared to their initial structures.

⚠ Attention:

- The modification patterns of STQ results are inverse to the normal theoretical calculation (and experimental), while the latter contains the effect of selection bias.
- *We can conclude that the selection bias covers the real intra-jet-broadening nature and leads to the narrowing modification of ΔR_{axis} distribution.*

Influence of Increased Quark-Jets

⚠ The STQ method obscures the quark-initiated jets increase effect that existed in experiments or conventional Monte Carlo studies.

Influence of Increased Quark-Jets

The STQ method obscures the quark-initiated jets increase effect that existed in experiments or conventional Monte Carlo studies.

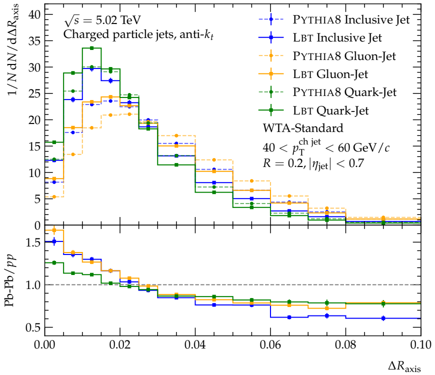

Figure: Normalized ΔR_{axis} distributions of the quark-jets, gluon-jets and inclusive jets in p+p and Pb+Pb collisions. ARXIV:2312.15518 [hep-ph]

Influence of Increased Quark-Jets

⚠ The STQ method obscures the quark-initiated jets increase effect that existed in experiments or conventional Monte Carlo studies.

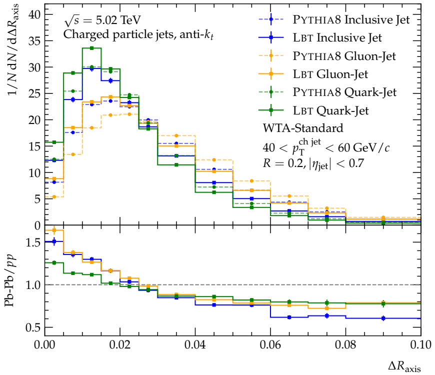

Figure: Normalized ΔR_{axis} distributions of the quark-jets, gluon-jets and inclusive jets in p+p and Pb+Pb collisions. arXiv:2312.15518 [hep-ph]

Conclusions:

- The quark-jets exhibit a narrower initial ΔR_{axis} distribution than the gluon-jets
- In Pb+Pb collisions, both the quark-jets and gluon-jets become narrower than in p+p

Influence of Increased Quark-Jets

⚠ The STQ method obscures the quark-initiated jets increase effect that existed in experiments or conventional Monte Carlo studies.

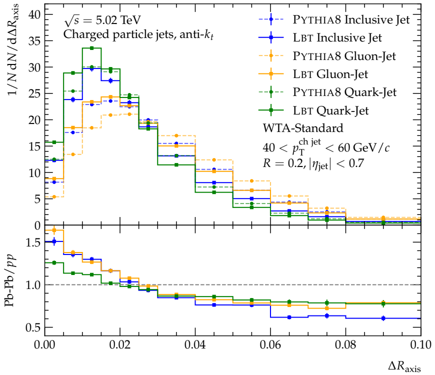

Figure: Normalized ΔR_{axis} distributions of the quark-jets, gluon-jets and inclusive jets in p+p and Pb+Pb collisions. arXiv:2312.15518 [hep-ph]

Conclusions:

- The quark-jets exhibit a narrower initial ΔR_{axis} distribution than the gluon-jets
- In Pb+Pb collisions, both the quark-jets and gluon-jets become narrower than in p+p

In p+p collisions, the fractions of quark-initiated jets and gluon-initiated jets are 36.7% and 63.3%, respectively.

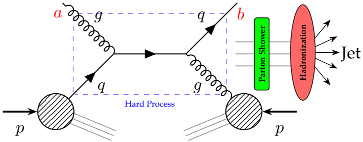

If the angular distance between a and j_1 is less than that between b and j_1, we identify j_1 as a gluon-jet.

Influence of Increased Quark-Jets

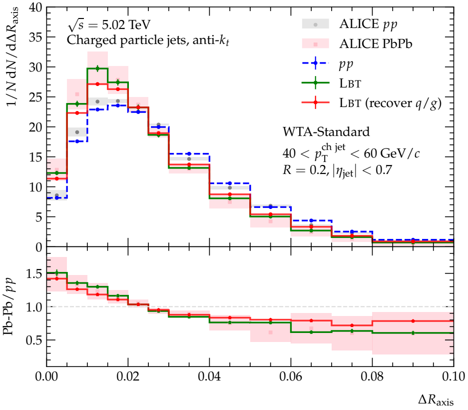

arXiv:2312.15518 [hep-ph]

Figure: The LBT calculations of ΔR_{axis} distributions in Pb+Pb collisions with recovered quark/gluon-jet fractions are compared with the normal LBT calculations and the ALICE data.

Conclusions:

- The calculations with rescaled fractions do not significantly differ from the normal LBT calculations
- The decreased gluon-jet fraction is **not** the main reason that leads to a narrowing ΔR_{axis} distribution of inclusive jet in Pb+Pb collisions

Matched UnQuenched Jets

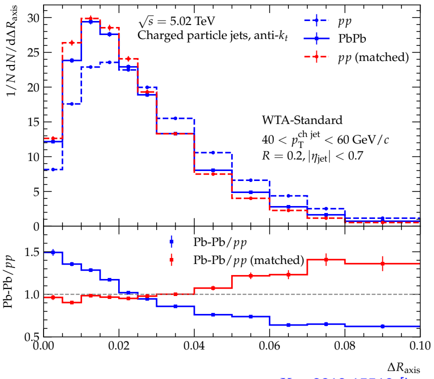

arXiv:2312.15518 [hep-ph]

Figure: The ΔR_{axis} distribution of the selected jet sample with p_T between 40 and 60 GeV in Pb+Pb collisions is compared to its initial counterpart, denoted as pp (matched), and that selected in *p*+*p* collisions.

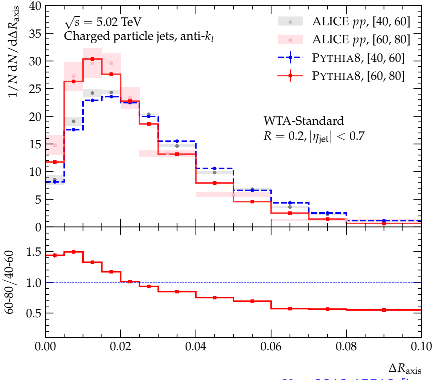

arXiv:2312.15518 [hep-ph]

Figure: Distributions of the ΔR_{axis} of inclusive jets calculated by the PYTHIA in *p*+*p* collisions within two different p_T intervals, and compared to the ALICE data.

Matched UnQuenched Jets

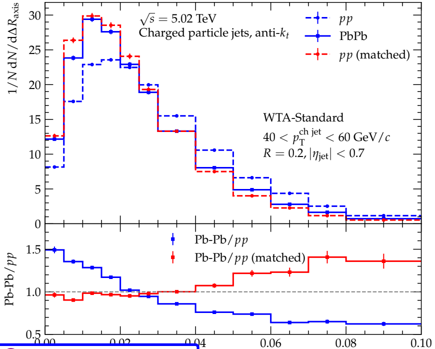

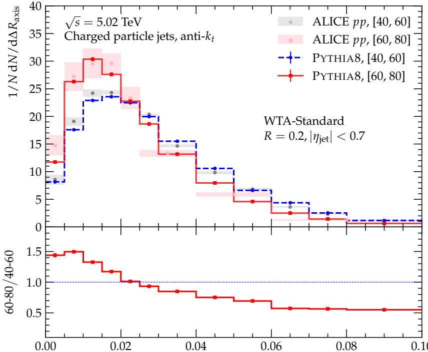

Conclusions

- The pp (matched) has a significantly narrower distribution than the $p+p$
- The jet sample selected in A+A collisions after jet quenching usually has higher initial p_T, while the one with higher p_T usually has narrower ΔR_{axis}
- The biased comparison between $p+p$ and A+A conceals the actual intra-jet-broadening effect

Summary

Highlights

- Utilizing a matching-jet method to track the jet evolution in the QGP to remove the selection bias in the Monte Carlo simulations, we observe that the ΔR_{axis} distribution becomes broader due to the jet-medium interactions
- By rescaling the quark/gluon-jet fractions in Pb+Pb collisions to be the same as that in p+p, we find that the fraction change may not significantly influence the modification pattern of jet ΔR_{axis}
- The selected jet sample in A+A collisions has a significantly narrower initial ΔR_{axis} distribution than the p+p baseline, and such a biased comparison between p+p and A+A conceals the actual jet-broadening effect in the experimental measurements

Outlook

- Use Z/γ-tagged jets to study the medium modification of the jet axis angle in heavy-ion collisions, thereby **reducing** the jet selection bias and **including** nPDF effects

Thank you for your attention!